TECHNICAL ARTICLE

Nanocrystalline and stacking-disordered β-cristobalite $AlPO_4$: the now deciphered main constituent of a municipal sewage sludge ash from a full-scale incineration facility

B. Peplinski,[1,a)] C. Adam,[1] B. Adamczyk,[1] R. Müller,[1] M. Michaelis,[1] T. Krahl,[2] and F. Emmerling[1]
[1]*BAM Federal Institute for Materials Research and Testing, Berlin, Germany*
[2]*Humboldt-Universität zu Berlin, Berlin, Germany*

(Received 23 September 2014; accepted 4 November 2014)

For the first time evidence is provided that a nanocrystalline and stacking-disordered, chemically stabilized β-cristobalite form of $AlPO_4$ occurs in a sewage sludge ash (SSA). This proof is based on a combined X-ray powder diffraction and X-ray fluorescence investigation of an SSA produced at a large-scale fluidized bed incineration facility serving a catching area with a population of 2 million. The structural and chemical characterization was carried out on 'as received' SSA samples as well as on solid residues remaining after leaching this SSA in sodium hydroxide solution. Thus, it was ascertained that the observed nanocrystalline and stacking-disordered cristobalite-like component belongs to the aluminum phosphate component of this SSA, rather than to its silicon dioxide component. In addition, a direct proof is presented that the chemically stabilized β-cristobalite form of $AlPO_4$ does crystallize from X-ray amorphous precursors under conditions that mimic the huge heating rate and short retention time (just seconds at $T \approx 850$°C), typical for fluidized bed incinerators.
 [doi:10.1017/S0885715614001213]

Key words: aluminum phosphate, chemical stabilization of high-temperature forms, cristobalite form, stacking disorder, incinerator ash, sewage sludge ash

I. INTRODUCTION

Sewage sludge and sewage sludge ashes (SSAs) are valuable secondary raw materials for phosphorus recovery. The correct identification of the main phosphorus-bearing mineral components in SSAs is highly desirable, e.g. for correct mass balance calculations of the P-component in SSAs that are, among others, needed for the optimization of P-recovery techniques. However, nothing was known about the crystal structure of the aluminum phosphate ($AlPO_4$) component in SSAs till the chemically stabilized high-temperature (HT) tridymite form of $AlPO_4$ was discovered in municipal SSA, produced at two European fluidized bed incineration facilities (Peplinski *et al.*, 2011, 2013). The SSAs from these two incinerators are probably not representative for the majority of SSAs, but the accompanying investigations into the (primary) crystallization of this special $AlPO_4$ form from well-defined amorphous precursors lead to results that are highly relevant for the structure characterization of municipal SSAs in general. These X-ray powder diffraction (XRD) investigations carried out at ambient by the present authors revealed that, the primary (nano)crystals formed at about 850 °C are heavily stacking-disordered hexagonal HT-tridymite and that their stacking fault density can be effectively reduced by heating them up to temperatures well above the primary crystallization. The discovery of stacking-disorder effects naturally raised the question about the nature of the other $AlPO_4$ forms belonging to the same polytype family as these are also likely to occur in SSAs. The most obvious candidate is the cubic β-cristobalite form that is thermodynamically stable above 200 °C (Wright and Leadbetter, 1975; Graetsch, 2003). Interestingly, XRD investigations carried out at ambient in a different context provided ample evidence that the SSA from a third fluidized bed mono-incineration facility contains a crystalline aluminum phosphate component with a so far unidentified crystallographic structure (Petzet *et al.*, 2011, 2012). This $AlPO_4$ component shows two distinct features: It contributes only one intensive Bragg reflection to the overall diffraction pattern of the SSA and the position of this reflection is at 21.4° (Cu$K\alpha$), i.e. only 0.08° off the most intense 111 reflection of the cubic β-cristobalite HT-form of $AlPO_4$ measured at 200 °C (Graetsch, 2003) but more than 0.3° off the position of the most intensive 111 reflection of the orthorhombic α-cristobalite form of $AlPO_4$ measured at room temperature (Graetsch, 2003) and PDF 00-011-500 (Swanson *et al.*, 1960; ICDD, 2013). On these two grounds it appeared reasonable to test whether the HT β-cristobalite form of $AlPO_4$ might be present in technical SSAs even at room temperature, i.e. in a chemically stabilized form. Such quest is all the more well-founded, as there are close relationships between the crystallographic structures of many $AlPO_4$-phases and their SiO_2-analogs – and it is well documented that the HT β-cristobalite form of SiO_2 can be chemically stabilized down to room temperature (Perrotta *et al.*, 1989).

Before embarking on an elaborate endeavor like this, it is productive to consider some of the obstacles that are likely to be encountered (and that possibly can explain why the occurrence of the cristobalite form of $AlPO_4$ has been overlooked in SSAs so far). First, although the existence of the HT

[a)]Author to whom correspondence should be addressed. Electronic mail: burkhard.peplinski@bam.de

β-cristobalite form of $AlPO_4$ is well established by HT XRD (Wright and Leadbetter, 1975; Graetsch, 2003), to the best of our knowledge there are no reports on a chemically stabilized form of this phase. Thus, it was not at all clear, how such a chemically stabilized substance might be synthesized. *Second*, the cubic HT cristobalite and the hexagonal HT-tridymite forms belong to the same polytype family. Their crystallographic structures are built from the layers of (nearly) identical structure and chemical composition and differ only in the stacking mode of these layers (for a detailed description see Graetsch and Flörke (1991)). Therefore it is more than likely, that a chemically stabilized HT cristobalite form of $AlPO_4$ that crystallized under the peculiar temperature-time regime, typical for fluidized bed incinerators is heavily affected by stacking disorder. Consequently, its diffraction pattern might considerably differ from the powder pattern (simulated on the basis of the structure data) of the perfectly crystallized HT-cristobalite form of chemically pure and stoichiometric $AlPO_4$. Third, the diffraction pattern of the cubic β-cristobalite form shows only few diffraction lines with sufficiently high (relative) intensity to be identified in a complex diffraction pattern of phase mixtures such as SSAs. Fourth, the diffraction patterns of the β-cristobalite form of $AlPO_4$ and SiO_2 are very similar and practically indistinguishable from each other in a complex phase mixture, even more if they are poorly crystallized.

A promising approach to alleviating some of the above-mentioned problems is to analyze a suitable SSA not only in the 'as received' state but to include additional samples produced from the 'as received' SSA through a series of selective dissolution pre-treatments. Alkaline leaching is especially well suited for this, as at pH values well above pH = 7 calcium phosphates and the cristobalite form of SiO_2 are practically insoluble while the solubility of $AlPO_4$ (and of some other components) is sufficiently high. Thus, the detrimental influence of peak overlap is reduced and it can be ascertained, whether the contribution of any β-cristobalite-like component to the overall diffraction pattern is indeed caused by an $AlPO_4$-component, rather than by SiO_2.

II. EXPERIMENTAL METHODS

A. Samples

The present investigation is focused on the structural and chemical investigation of SSA "F–S" produced at a large-scale fluidized bed incineration facility in Europe serving a catching area with a population of two million. This incinerator is located in a municipality different from those where the previously investigated SSAs "Md2" and "D" came from. The chemical composition of these three SSAs is given in Table I. Differences are mainly observed for the elements magnesium, aluminum, phosphorus, potassium, and iron. This X-ray fluorescence (XRF) data are in full agreement with the results of ICP–OES analyses (not shown).

The crystallographic and chemical characterization of SSA "F–S" involved five samples: the 'as received' SSA and four leaching residues, resulting from a series of four consecutive alkaline leaching treatments. This SSA was subjected to the first alkaline leaching that was carried out as follows: 50 g of the 'as received' SSA "F–S" were suspended in 1 liter of 0.5% sodium hydroxide solution. The suspension was stirred with a magnetic mixer at room temperature. After 30 min the stirrer was switched off and after 3 h the liquid was decanted and the settled solid residue was filtrated and pH-controlled washed in demineralized water. After drying at 105 °C, a sub-sample of 10 g was taken for XRD and XRF analyses. The whole remaining residue was subjected to a second leaching following a very similar procedure using 1.0% sodium hydroxide solution and a solid-to-liquid ratio of 1:26. For the third and fourth leaching, 2.0% sodium hydroxide solution and a solid-to-liquid ratio of 1:40 were applied. Thus, a set of four residues were produced for X-ray analyses. Each of these four residues represents another of the intermediate states of the chemical and mineralogical composition of SSA "F–S" which is stripped off its alkaline-soluble components step by step by repeating the leaching.

In addition to the samples gained from the industrially produced SSA, a series of model samples of the chemically stabilized β-cristobalite form of $AlPO_4$ was synthesized under well-defined laboratory conditions and was analyzed. These synthetic model substances were crystallized by heating an X-ray amorphous non-stoichiometric and doped aluminum phosphate precipitate ($Me_x^{2+}Al_{1+x}^{3+}P_{1-x}^{5+}O_4$) to 876 °C, holding at this temperature for < 10 s and then quenching it to room temperature. This (T,t)-program was realized by fast inserting 35 mg of the precursor substance into a preheated horizontal tube furnace and – after a short retention time – fast withdrawing the heat-treated substance. Twenty repetitions of this procedure produced a sufficiently large pooled sample. This experimental set-up (Peplinski *et al.,* 2013) allows not only accurate temperature control of the entire sample but also sample heating rates of up to 1000 ° min^{-1} and thus mimics quite well the (T,t)-conditions expected for industrial sewage sludge incinerators of the fluidized bed type.

B. Specimen preparation

All SSA samples analyzed by XRD and XRF were first pulverized and homogenized for 60 s in a vibratory disc mill using a tungsten carbide grinding set. SSA specimens for XRD analyses had a diameter of 38 mm, and a thickness of 1 mm. For the XRD analysis of the model samples of the chemically stabilized β-cristobalite form of $AlPO_4$ synthesized under well-defined laboratory conditions, a low background specimen holder with Ø 20 mm × 0.5 mm sample cavity was used. For precise line position determinations quartz powder was used as an internal standard.

Before being analyzed by XRF, the ground SSA powders as well as the model sample of the chemically stabilized β-cristobalite form of $AlPO_4$ were compressed into the shape of dense solid discs having a diameter of 32 mm and a height of 4 mm.

C. Data collection

XRD measurements were performed at room temperature on a Bruker-AXS D5000 diffractometer in Bragg-Brentano geometry using an 1.0 mm aperture, a 0.1 mm receiving slit, a sample spinner (0 or 15 rpm), and an Si(Li) solid-state detector. Data were collected in the 2Θ-range from 5° to 80° in steps of 0.02° for 40 s per step, using copper $K\alpha_{1,2}$ radiation with 40 kV × 30 mA. X-ray fluorescence analyses (XRF) were carried out with a MagiXPro instrument (Panalytical) equipped with a sealed rhodium tube operated at 60 kV × 60 mA and with Bragg crystal analyzer.

https://doi.org/10.1017/S0885715614001213 Published online by Cambridge University Press

TABLE I. Abundance of the main chemical components in the 'as received' raw SSAs "F–S", "Md2" and "D", according to XRF analysis.

SSA	Mass fractions (wt.%)													
	O	Na	Mg	Al	Si	P	S	K	Ca	Ti	Mn	Fe	Cu	Zn
F–S	47.6	0.5	1.0	12.7	10.8	8.8	0.6	0.8	12.3	0.5	0.1	2.3	0.2	0.3
Md2	49.1	0.6	2.0	7.2	8.0	11.2	1.3	2.0	13.8	0.4	0.1	3.7	0.2	0.3
D	45.2	0.7	2.4	3.9	11.0	11.8	0.4	2.1	9.2	0.7	0.2	11.3	0.1	0.3

III. RESULTS and DISCUSSION

Sections of the XRD patterns collected before the first and after the second, third, and fourth alkaline leaching of SSA "F-S" are given in Figures 1–3. These data is represented by blue curves with circles. For comparison, a red solid curve shows the room-temperature diffraction pattern of a nanocrystalline and stacking-disordered model sample of the chemically stabilized cubic β-cristobalite HT-form of $AlPO_4$, synthesized under well-defined laboratory conditions as described at the end of the SAMPLE section. The 111 reflection of the β-cristobalite form at about 21.4° is well discernible in this diffraction pattern and the 220 reflection at about 35.4° as well. The shape of the broad 19.5–24.5° band in the observed diffraction patterns of the synthetic $AlPO_4$ model sample, fits very well the intensity distribution of published simulated powder patterns calculated for β-cristobalite crystals randomly interstratified with HT-tridymite layers assuming nearly equal probabilities for the cubic and the hexagonal stacking sequences, i.e. for heavily stacking-disordered β-cristobalite (Graetsch *et al.*, 1994; Guthrie *et al.*, 1995). The agreement between the observed diffraction patterns of our model $AlPO_4$ samples and the published simulated patterns even further improves if the structure model used for the simulation includes a small degree of ordered stacking as this leads to a slight shoulder at the high-angle side of the 19.5–24.5° band (Guthrie *et al.*, 1995). Such coherent intergrowth of lamella with cristobalite and tridymite stacking sequences has previously been ascertained by different scanning calorimetry, the X-ray precession method, and nuclear magnetic resonance (NMR), and it was directly visualized by transmission electron microscopy (TEM) (Elzea and Rice, 1996). According to Thomas *et al.* (1994), the formation of an occasional $AlPO_4$ tridymite stacking faults within cristobalite crystals suppresses

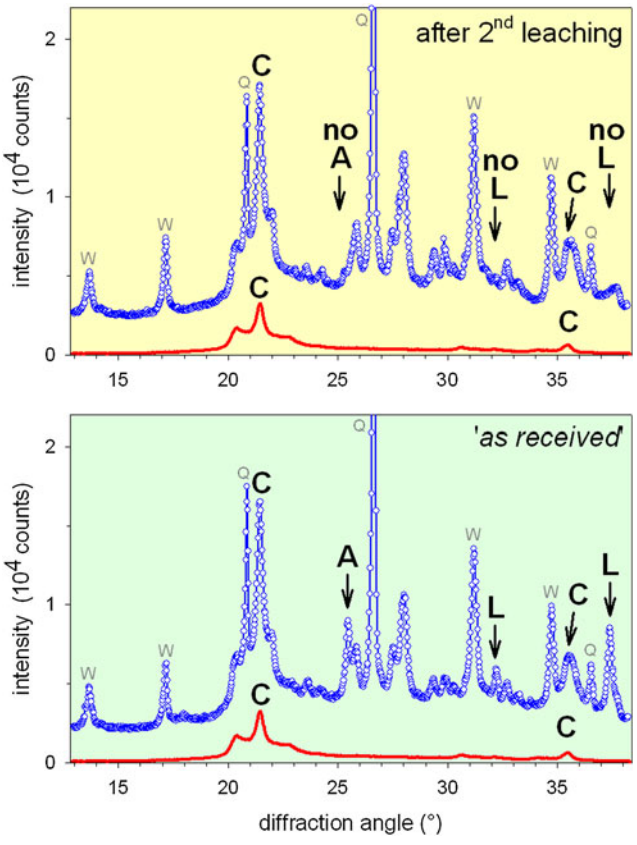

Figure 1. (Color online) Sections of the diffraction patterns of SSA "F–S" 'as received' (bottom) and after the second (top) alkaline leaching (blue curves with circles) and of the nanocrystalline and stacking-disordered model sample of the chemically stabilized cubic β-cristobalite form of $AlPO_4$ measured at room temperature (red solid curve). A, anhydrite; C, β-cristobalite form; L, lime; Q, quartz; W, whitlockite type.

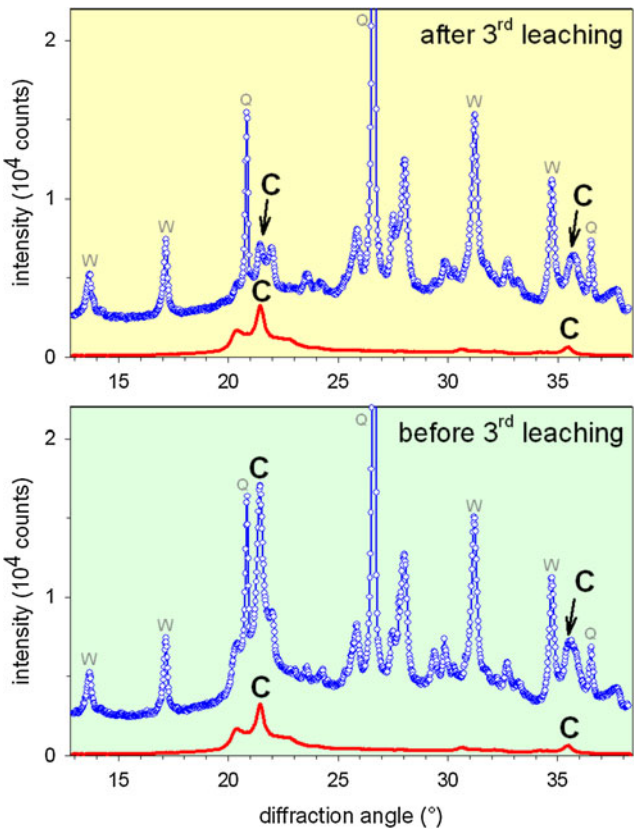

Figure 2. (Color online) Sections of the diffraction patterns of SSA "F–S" before (bottom) and after (top) the third alkaline leaching (blue curves with circles) and of the nanocrystalline and stacking-disordered model sample of the chemically stabilized cubic β-cristobalite form of $AlPO_4$ measured at room temperature (red solid curve). The letter "C" indicates the presence of a diffraction line of the β-cristobalite form.

https://doi.org/10.1017/S0885715614001213 Published online by Cambridge University Press

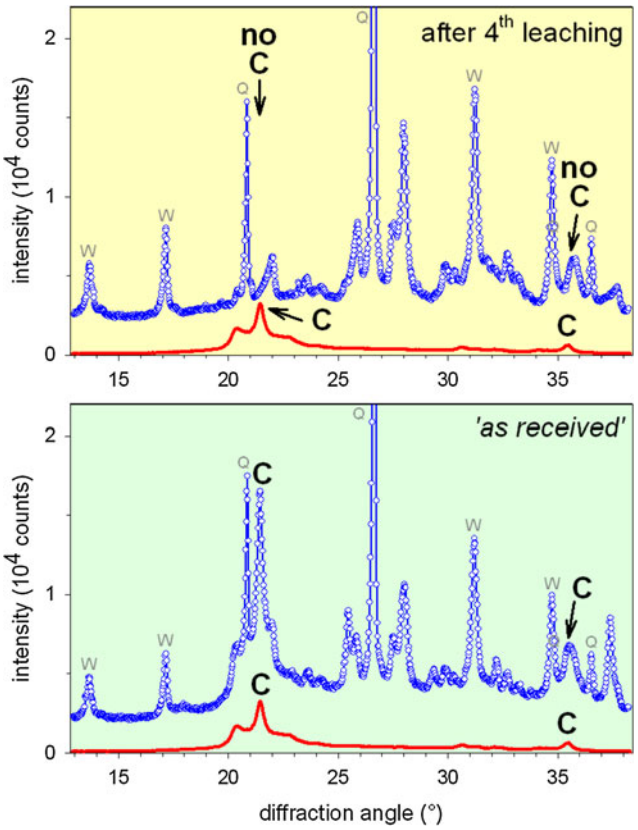

Figure 3. (Color online) Sections of the diffraction patterns of SSA "F–S" 'as received' (bottom) and after the fourth (top) alkaline leaching (blue curves with circles) and of the nanocrystalline and stacking-disordered model sample of the chemically stabilized cubic β-cristobalite form of $AlPO_4$ measured at room temperature (red solid curve). C, β-cristobalite form; Q, quartz; W, whitlockite type.

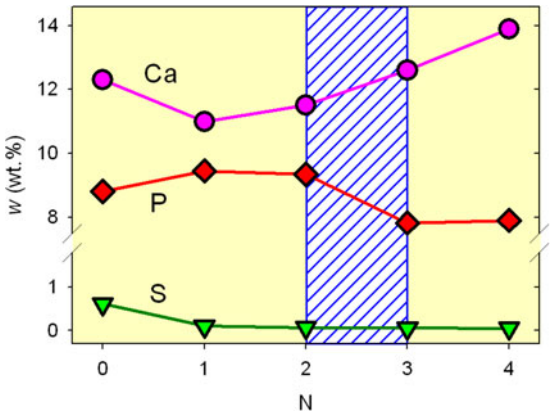

Figure 4. (Color online) Chemical composition of SSA "F–S" in dependence on N, the number of the applied alkaline leaching treatments. XRF data.

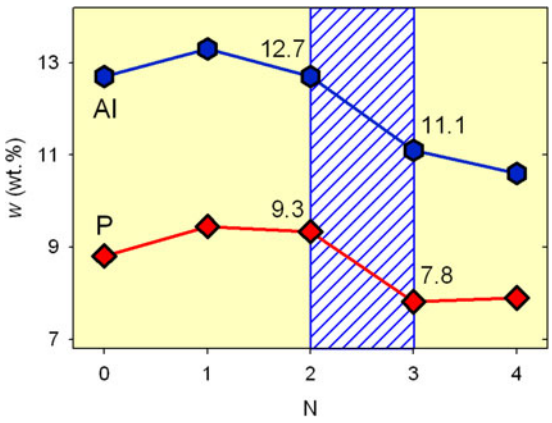

Figure 5. (Color online) as Figure 4.

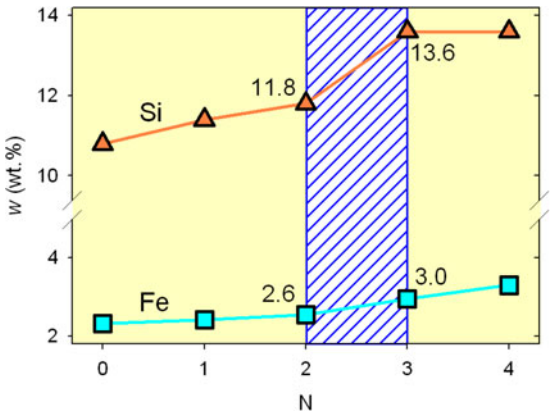

Figure 6. (Color online) as Figure 4.

the β- → α-cristobalite phase transition, i.e. stabilizes the cubic HT β-cristobalite structure down to room temperature.

The foregoing remarks on the synthetic model samples can be equally applied to the diffraction pattern of the 'as received' SSA "F–S", provided, that the following points are not ignored: In the diffraction pattern of SSA "F–S", the β-cristobalite diffraction line profiles partially overlap with reflections of alkaline-insoluble phases (quartz, silicates, and calcium phosphate). Thus, the high-angle side of the 111 reflection of the β-cristobalite form at about 21.4° is distorted by a low-intensity reflection centered at about 22.0° and belonging to an alkaline-insoluble component (see upper halves of Figures 2 and 3). Similarly, the lower-intensity 220 reflection of the β-cristobalite form at about 35.4° partially overlaps with a reflection centered at 35.8° that has comparable peak-height and line-width and belongs to an alkaline-insoluble component. Despite this partial overlap, the drop of intensity of the 220 reflection caused by the alkaline dissolution treatment is clearly seen in the zoomed diffraction patterns.

Figures 4–6 depict the results of the XRF analyses for SSA "F–S" in dependence on N, the number of the applied alkaline leaching treatments.

Figure 1 shows that the first two alkaline leaching treatments of SSA "F–S" cause a complete disappearance of the Bragg reflections of two components: $CaSO_4$ (anhydrite) and CaO (lime). Furthermore, there are subtle changes in the diffraction pattern: the intensity of the Bragg reflections of $(Ca,Mg)_3(PO_4)_2$ (whitlockite-type) and of calcite ($CaCO_3$) slightly increases, simultaneously, broadened reflections of nanocrystalline hydroxyl-apatite appear, while the diffracted intensity of the β-cristobalite form remains essentially unchanged. These findings are reflected in the XRF results for $N = 0 \rightarrow N = 2$ as depicted in Figures 4–6: The mass fraction of only one element, sulfur, shows a steep fall down to zero and the mass fraction of calcium decreases by about 1 wt.%.

https://doi.org/10.1017/S0885715614001213 Published online by Cambridge University Press

At the same time the abundance of aluminum remains in summa unchanged (as the changes occurring during the first ($N = 1$) and the second ($N = 2$) leaching step are compensating each other), whereas the abundance of P, Si, and Fe increases.

Figure 2 documents that the third alkaline leaching of SSA "F–S" leads to a very significant reduction in the diffracted intensity of the nanocrystalline and stacking-disordered β-cristobalite form, whereas the corresponding XRF data given in Figures 4–6 show a considerable reduction of the abundance of only two elements: phosphorus and aluminum, whereas the mass fractions of silicon, iron, and calcium (and many other elements not shown in this graphic) increase at the same time. Thus it is proved beyond doubt that the dissolved nanocrystalline and stacking-disordered β-cristobalite form in SSA "F–S" is indeed an $AlPO_4$ phase, but not SiO_2.

Figure 3 shows that after the fourth alkaline leaching even the last remains of the nanocrystalline and stacking-disordered β-cristobalite form of $AlPO_4$ are gone.

In an additional investigation, the internal standard method and line profile fitting were applied to determine the line position of the 111 Bragg reflection of the β-cristobalite form at about 21.4° precisely, both for SSA "F–S" as well as for the nanocrystalline and stacking-disordered model sample of the chemically stabilized cubic β-cristobalite form of $AlPO_4$ synthesized under well-defined laboratory conditions. These two results agree within ±0.005°.

IV. CONCLUSION

XRD and XRF data for the first time provide evidence for the occurrence of a nanocrystalline and stacking-disordered, chemically stabilized β-cristobalite form of $AlPO_4$ in an SSA.

In addition, the diffraction pattern of a model substance synthesized under well-defined laboratory conditions proves that a nanocrystalline and stacking-disordered, chemically stabilized β-cristobalite form of $AlPO_4$ does crystallize from X-ray amorphous precursors at 876 °C in <10 s, i.e. under (T,t)-conditions that mimic quite well those inside the incinerator used for the production of the investigated SSA – although in chemically pure and stoichiometric $AlPO_4$ (or SiO_2) precursors, the crystallization of the cristobalite form is sluggish even at much higher temperatures.

Elzea, J. M. and Rice, S. B. (**1996**). "TEM and X-ray diffraction evidence for cristobalite and tridymite stacking sequences in opal," Clay Clay Miner. **44**, 492–500.

Graetsch, H. and Flörke, O. W. (**1991**). "X-ray powder diffraction patterns and phase relationship of tridymite modifications," Z. Kristallogr. **195**, 31–48.

Graetsch, H., Gies, H., and Topalovic, I. (**1994**). "NMR, XRD and IR study of microcrystalline opals," Phys. Chem. Miner. **21**, 168–175.

Graetsch, H. A. (**2003**). "Thermal expansion and thermally induced variations of the crystal structure of $AlPO_4$ low cristobalite," N. Jb. Miner. Mh., Jg. **2003**(7), 289–301.

Guthrie, G. D., Bish, D. L., and Reynolds, R. C. (**1995**). "Modelling the X-ray diffraction pattern of opal-CT," Am. Mineral. **80**, 869–872.

ICDD (**2013**). PDF-4+ 2013 (Database), edited by . Soorya Kabekkodu, International Centre for Diffraction Data, Newtown Square, PA, USA.

Peplinski, B., Adam, C., Reuther, H., Vogel, C., Adamczyk, B., Menzel, M., Emmerling, F., and Simon, F.-G. (**2011**). "First identification of the tridymite form of $AlPO_4$ in municipal sewage sludge ash," Z. Kristallogr. Proc. **1**, 443–448.

Peplinski, B., Adam, C., Adamczyk, B., Müller, R., Schadrack, R., Michaelis, M., Emmerling, F., Reuther, H., and Menzel, M. (**2013**). "Evidence of formation of the tridymite form of $AlPO_4$ in some municipal sewage sludge ashes," Powder Diffr. J. **28**(S2), S425–S435.

Perrotta, J. A., Grubbs, D. K., Martin, E. S., Dando, N. R., McKinstry, H. A., and Huang, C.-Y. (**1989**). "Chemical stabilization of β-cristobalite," J. Am. Ceram. Soc. **72**, 441–447.

Petzet, S., Peplinski, B., Bodkhe, S. Y., and Cornel, P. (**2011**). "Recovery of phosphorus and aluminium from sewage sludge ash by a new wet chemical elution process (SESAL-Phos-recovery process)," Water Sci.Technol. **64**, 693–699.

Petzet, S., Peplinski, B., and Cornel, P. (**2012**). "On the wet chemical phosphorus recovery from sewage sludge ashes by acidic or alkaline leachings and by an optimized combination of both," Water Res. **46**, 3769–3780.

Swanson, H. E., Cook, M. I., Evans, E. H., and deGroot, J. H. (**1960**). "Aluminum orthophosphate, $AlPO_4$ (orthorhombic)," Natl. Bur. Stand. (U.S.) Circ. **539**, Standard X-ray Diffraction Powder Patterns, **10**, 4–6.

Thomas, E. S., Thompson, J. G., Withers, R. L., Sterns, M., Xiao, Y., and Kirkpatrick, R. J., (**1994**). "Further investigation of the stabilization of β-cristobalite," J. Am. Ceram. Soc. **77**, 49–56.

Wright, A. F. and Leadbetter, A. J. (**1975**). "The structure of the β-cristobalite phases of SiO_2 and $AlPO_4$," Philos. Mag. **31**, 1391–1401.

https://doi.org/10.1017/S0885715614001213 Published online by Cambridge University Press